Letter

Enhancing spin squeezing using soft-core interactions

Jeremy T. Young , 1,2,* Sean R. Muleady , 1,2 Michael A. Perlin , 1,2 Adam M. Kaufman, 1 and Ana Maria Rey , 1,2

1 JILA, University of Colorado and National Institute of Standards and Technology, and Department of Physics, University of Colorado, Boulder, Colorado 80309, USA

2 Center for Theory of Quantum Matter, University of Colorado, Boulder, Colorado 80309, USA



(Received 25 August 2022; revised 8 December 2022; accepted 8 February 2023; published 10 March 2023)

We propose a protocol for preparing spin squeezed states in controllable atomic, molecular, and optical systems, with particular relevance to emerging optical clock platforms compatible with Rydberg interactions. By combining a short-range, soft-core potential with an external drive, we can transform naturally emerging Ising interactions into an XX spin model while opening a many-body gap. The gap helps maintain the system within a collective manifold of states where metrologically useful spin squeezing can be generated. We examine the robustness of our protocol to experimentally relevant decoherence and show favorable performance over typical protocols lacking gap protection. For example, in a 14×14 system, we observe that soft-core interactions can generate spin squeezing comparable to an all-to-all Ising model even in the presence of relevant decoherence, the same amount of squeezing as the decoherence-free XX spin model with $1/r^3$ dipolar interactions, and a 5.8 dB gain over the decoherence-free XX spin model with $1/r^6$ interactions.

DOI: 10.1103/PhysRevResearch.5.L012033

As the control of quantum systems has progressed in recent decades, so too has the ability to create and harness quantum entanglement for improved quantum technology. In the context of quantum sensors, this entails applying entangled resources to increasingly push beyond the standard quantum limit (SQL)—the fundamental noise floor for uncorrelated particles—towards the fundamental limits imposed by quantum mechanics [1-5]. Although current state-of-the-art optical clocks provide some of the most precise measurements in physics [6–9], they will eventually reach a point where improvements in sensing capabilities based on uncorrelated atoms have diminishing returns due to both fundamental and practical constraints. In light of this, the utilization of entanglement provides an additional axis for optimization, which will be crucial for the next generations of optical clocks once the limits of these constraints are reached.

In recent years, tweezer arrays of neutral atoms have emerged as a promising new platform for optical clocks [10–12], driven by a number of recent advances, including the rapid preparation of tunable arrays with high filling fractions and single-atom control [13–18] and half-minute-scale coherence times on optical clock transitions [11,12]. Such platforms combine the control and high-duty cycles of ion clocks [9,19,20] with the scalability of optical lattice clocks [6,7] while mitigating their respective drawbacks, such as interatomic collisions in lattice clocks or large shot noise in

Published by the American Physical Society under the terms of the Creative Commons Attribution 4.0 International license. Further distribution of this work must maintain attribution to the author(s) and the published article's title, journal citation, and DOI.

ion clocks. Moreover, in these systems, tunable Ising interactions via Rydberg states [21–24] that decay as $1/r^{\alpha}$ with interparticle distance r offer a natural avenue for generating metrologically useful entanglement in the form of spin squeezing [25–27].

For Ising interactions, as long as the dimension of the array $D \leq \alpha$, the power-law interactions provide only a small, constant noise reduction that is independent of particle number [28]. Power-law XXZ models have also been explored theoretically as a way to further enhance spin squeezing due to the presence of a many-body gap [29,30]. However, the theoretical squeezing enhancement is limited for $1/r^6$ van der Waals (vdW) interactions in two dimensions (2D), while $1/r^3$ dipolar interactions cannot be extended to 3D due to their angular dependence. Moreover, the generation of both $1/r^{\alpha}$ vdW and dipolar interactions requires direct excitation to the Rydberg state(s). As a result, the spin squeezing will be generated on a Rydberg transition. However, in order to utilize the squeezing for quantum-enhanced metrology, the squeezing must be encoded in a pair of long-lived states, such as on a clock transition. Transferring the squeezing from the Rydberg state(s) to the long-lived states will introduce additional noise, reducing the squeezing and limiting the metrological gain.

We propose to utilize a strong transverse field in combination with a soft-core potential, realizable with Rydberg dressing, to generate strongly collective dynamics which are protected by a many-body gap (see Fig. 1) [29–44]. Our proposal dramatically extends the system sizes for which the optimal spin squeezing mimics that of a fully collective Ising model, also known as the one axis twisting (OAT) model [25,45]. For example, in a 2D system of 32×32 atoms, an interaction range of only three times the lattice spacing is needed to realize near-OAT squeezing, even though the number of atoms that fall within the soft-core potential is

^{*}Corresponding author: jeremy.young@colorado.edu

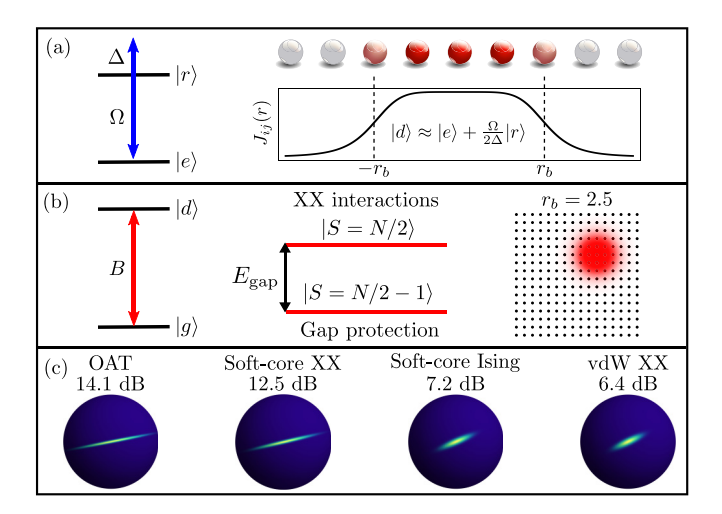


FIG. 1. Gap-protected spin squeezing with soft-core interactions. (a) The state $|e\rangle$ is weakly dressed with a Rydberg state $|r\rangle$ with Rabi frequency Ω and detuning Δ , resulting in a soft-core potential with blockade radius (i.e., range) r_b for the dressed state $|d\rangle$. (b) By applying a strong transverse field B via a drive between $|g\rangle$ and $|d\rangle$, the system realizes an approximate OAT Hamiltonian with an additional term which opens a gap $E_{\rm gap} \propto 2S$ between adjacent S manifolds. Combined with the soft-core potential, near-OAT squeezing can be realized even when the number of atoms within the blockade radius $N_b \ll N$, such as for $r_b = 2.5$ in a 14 × 14 lattice, where $N_b \approx N/10$. (c) Husimi distributions associated with the optimal squeezing for several protocols in a 14 × 14 lattice, with $r_b = 2.5$ for the soft-core interactions as in (b). While squeezing from soft-core XX interactions is comparable to that of OAT, the soft-core Ising and vdW XX models produce far less squeezing.

about 36 times smaller than the system size. Unlike power-law interactions, the protocol here generates squeezing between two long-lived states (e.g., on a clock transition) as a result of the Rydberg dressing [46]. Additionally, we show that in the presence of relevant decoherence in a 14×14 system, the protocol here generates the same amount of squeezing as a decoherence-free long-range $1/r^3$ (dipolar) XX model, and provides a 5.8 dB gain over a decoherence-free $1/r^6$ (vdW) XX model.

Model. We consider a scheme where a long-lived internal state $|e\rangle$ is dressed with a Rydberg state $|r\rangle$ via a drive with Rabi frequency Ω and detuning Δ [47–59]. The resulting dressed state $|d\rangle \approx |e\rangle + \frac{\Omega}{2\Delta}|r\rangle$ and a ground state $|g\rangle$ form the basis of an effective spin-1/2 system governed by the Hamiltonian

$$H = \sum_{i < i} J_{ij} (1/2 + s_i^z) (1/2 + s_j^z), \tag{1a}$$

$$J_{ij} = \frac{\Omega^4}{8\Delta^3} \frac{1}{1 + (r/r_b)^6}, \quad \frac{C_6}{r_b^6} = -2\Delta,$$
 (1b)

where $s_i^{\mu} \equiv \sigma_i^{\mu}/2$ denote the spin-1/2 operators at site i, J_{ij} is a soft-core potential with a range of blockade radius r_b and $1/r^6$ tail, and C_6/r^6 is the vdW interaction. Here, r_b is in units of the lattice spacing. Physically, we can understand the emergence of this Hamiltonian as follows: at large distances, the Rydberg states interact weakly, leading to a vdW tail with reduced strength f^2C_6 , where $f \equiv \Omega^2/4\Delta^2$ is the Rydberg

fraction. However, at short distances where $|C_6/r^6| \gg |2\Delta|$ (i.e., $r \ll r_b$), the excitation of more than one Rydberg atom is strongly suppressed due to blockade. As a result, the corresponding contribution to the light shift is suppressed, leading to a plateau of strength $J_0 \equiv 2\Delta f^2 = \Omega^4/8\Delta^3$. Finally, we note that in addition to the Ising interactions, Eq. (1a) contains an inhomogeneous longitudinal field. Unless otherwise noted, we shall assume that these terms can be neglected either via spin echo or a rotating wave approximation (RWA) in the presence of a strong drive, as discussed below (see Supplemental Material [60]).

An effective transverse field along the x direction can be generated by applying a drive which couples $|g\rangle$ and $|d\rangle$ with Rabi frequency B. In the limit of $B \gg (N-1)\overline{J} \equiv \frac{1}{N} \sum_{i,j} J_{ij}$ (see Supplemental Material [60]), where $(N-1)\overline{J}$ is the average interaction each atom feels, and in the frame of the applied transverse field, the Ising interactions take the form of XX interactions since, under the RWA, the fast oscillating terms can be dropped out. The final Hamiltonian takes the form of an XX model [61–66],

$$H_{\text{RWA}} = \frac{1}{2} \sum_{i < j} J_{ij} \left(s_i^y s_j^y + s_i^z s_j^z \right). \tag{2}$$

Note that in the course of making the RWA, the overall strength of the interactions has been reduced by a factor of two.

Enhanced squeezing. For a system of N spin-1/2 particles, the Wineland spin squeezing parameter ξ , defined as [26,27]

$$\xi^2 \equiv \frac{N \min{\langle \Delta S_{\perp}^2 \rangle}}{|\langle \mathbf{S} \rangle|^2},\tag{3}$$

quantifies the reduction in the phase uncertainty beyond the SQL of $1/\sqrt{N}$. Here, $\mathbf{S} \equiv \sum_i \mathbf{s}_i$, and $\min{\langle \Delta S_\perp^2 \rangle}$ denotes the minimum variance in directions perpendicular to the Bloch vector. To dynamically generate a spin squeezed state, we initially polarize all spins in the xy plane or yz plane for the Ising and XX models, respectively. The corresponding dynamics will squeeze the state until it reaches an optimal (i.e., minimal) value of $\xi_{\text{opt}}^2 \equiv \xi^2(t_{\text{opt}})$ after time t_{opt} . For Ising interactions, Rydberg dressing allows for an im-

For Ising interactions, Rydberg dressing allows for an improvement in $\xi_{\rm opt}^2$ over the power-law interactions inherent to Rydberg states [46]. This is because within a blockade radius, the interactions are all to all, and thus the model realizes an effective OAT Hamiltonian $H_{\rm OAT} \equiv \frac{\overline{J}}{2}S_z^2$ when the system size $N \lesssim N_b$, where N_b is the number of atoms within a blockade radius. The optimal spin squeezing accessible via OAT dynamics scales as $\xi_{\rm opt}^2 \sim N^{-2/3}$ in time $\overline{J}t_{\rm opt} \sim N^{-2/3}$ [25,45]. However, as we increase the system size $N \gtrsim N_b$, the deviation from the dynamics of $H_{\rm OAT}$ quickly becomes significant as the states $|S, m_z\rangle$, $|S', m_z\rangle$ with $S \neq S'$ become coupled (S denotes the total spin and m_α the projection onto S_α), which are decoupled in $H_{\rm OAT}$. Increasing the system size further leads to limited improvement in $\xi_{\rm opt}^2$. For vdW interactions, the presence of the $1/r^6$ tail in the soft-core potential does allow for a moderate enhancement over the naive estimate of $\xi_{\rm opt}^2 \sim N_b^{-2/3}$, and $\xi_\infty^2 \propto r_b^{-.76D} \propto N_b^{-.76}$ for $D \leqslant 3$ [46], where the ∞ subscript denotes $\xi_{\rm opt}^2$ in the large-N limit.

To understand how the squeezing behavior changes for the XX model, it is convenient to reexpress the Hamiltonian as

$$H_{\text{RWA}} = \frac{1}{2} H_{\text{gOAT}} + \frac{1}{2} \sum_{i \in i} (\overline{J} - J_{ij}) s_i^x s_j^x,$$
 (4a)

$$H_{\text{gOAT}} = \sum_{i < j} J_{ij} \mathbf{s}_i \cdot \mathbf{s}_j - \frac{\overline{J}}{2} S_x^2.$$
 (4b)

We see that the effective OAT Hamiltonian has an additional SU(2)-symmetric term. Although this is not a collective term, it nevertheless commutes with S^2 . As a result, this term will not couple different S manifolds, but it will break their degeneracy in the OAT model, leading to a gapped OAT Hamiltonian H_{gOAT} . As in the Ising model, the squeezing dynamics of the XX model reduces to that of the OAT model for $N \lesssim N_b$. However, the presence of a gap between different S manifolds permits that as N is increased beyond N_b , the deviations from H_{gOAT} can be initially treated as a perturbation, extending the effective OAT-like behavior to larger N compared to Ising interactions and enhancing the attainable optimal squeezing.

To determine the degree of enhancement to $\xi_{\rm opt}^2$ from the soft-core potential, we study both models numerically. For the Ising model, this can be done exactly. However, for the *XX* model, this is no longer possible and we must rely on numerical approximations. We use the discrete truncated Wigner approximation (DTWA) [67–69], which shows good agreement with results using the time-dependent variational principle for matrix product states in 1D (see Supplemental Material [60]); analogous benchmarks in 2D for spin systems with power-law interactions exhibit similar agreement [70].

In Figs. 2(a) and 2(b), we compare ξ_{opt}^2 attainable in the XX model vs the Ising model. The XX model retains the OAT scaling $\xi_{\text{opt}}^2 \sim N^{-2/3}$ for system sizes well beyond the naive expectation of $N \sim N_b \approx \pi r_b^2$, while ξ_{opt}^2 for the Ising interactions saturates at much smaller system sizes in comparison. For example, for $r_b = 3$, corresponding to $N_b \approx 28$, ξ_{opt}^2 for Ising interactions begins to diverge from the comparable OAT results around N = 9. In contrast, for the XX interactions, ξ_{opt}^2 is only slightly reduced from the OAT result at $N = 1024 \approx 36N_b$. Additionally, we note that $r_b = 1$ provides a good approximation to pure $1/r^6$ vdW interactions, illustrating the importance of the soft-core potential to enhancing ξ_{opt}^2 .

To understand the scaling of $\xi_{\rm opt}^2$ with N_b , we define $N_{\rm OAT}$ as the number of atoms necessary for the OAT model to generate a state with optimal squeezing ξ_{∞}^2 , thus determining the system sizes for which OAT scaling persists. We also investigate the gap protection by investigating the behavior of $\langle S^2 \rangle / [N/2(N/2+1)]$, which provides a measure of how collective the system is. In particular, we identify $N_{0.95}$, the number of atoms at which $\langle S^2 \rangle / [N/2(N/2+1)] = 0.95$ at $t_{\rm opt}$. This scaling is presented in Figs. 2(c) and 2(d) for 1D and 2D with a sharp cutoff in the soft-core potential and periodic boundary conditions. We see that both indicate that OAT scaling for the Ising model persists to $N \propto N_b$ and is independent of the dimension, as expected. In contrast, OAT scaling for the XX model persists to $N \propto N_b^{3D/2}$, corresponding to $\xi_{\infty}^2 \propto N_b^{-D}$. Aside from the enhancement over Ising interactions, we see that the gap protection appears to be

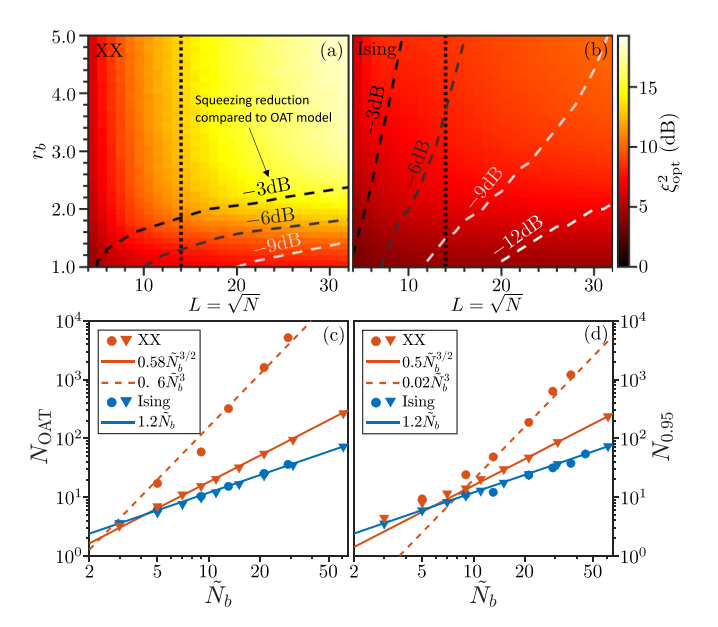


FIG. 2. We show the optimal squeezing generated as a function of r_b and the system side length L for 2D systems of size $N=L\times L$ for (a) the XX model and (b) the Ising model. The black dotted line corresponds to systems with L=14, for which we later consider the effects of decoherence. The dashed contours denote the reduction in $\xi_{\rm opt}^2$ for each model compared to that of an OAT model for N particles. (c) Scaling of effective OAT atom number $N_{\rm OAT}$ associated with ξ_{∞}^2 for 1D (triangles) and 2D (circles) for a potential with a sharp cutoff as a function of $\tilde{N}_b \equiv N_b + 1$. (d) Scaling of $N_{0.95}$ (N at which $\langle S^2 \rangle / [N/2(N/2+1)] = 0.95$ at $t_{\rm opt}$) as a function of \tilde{N}_b . Lines are meant to illustrate the scaling and are not fits.

stronger at higher dimensions, leading to a further enhancement in the OAT scaling. Furthermore, we note that these calculations are done for a constant soft-core potential with no power-law tail, indicating that the physics we identify here is not a consequence of the power-law tail.

Finally, let us discuss the behavior of the squeezing time. When $N \lesssim N_b$, $\overline{J} \approx J_0$, so the squeezing time scales like $J_0 t_{\rm opt} \approx \overline{J} t_{\rm opt} \sim N^{-2/3}$. However, for $N > N_b$, we have $\overline{J} \approx J_0 N_b/N$, and the squeezing time scales like $J_0 t_{\rm opt} \sim N^{1/3}/N_b$, leading to a tradeoff between enhanced squeezing and shorter squeezing times, which can become particularly important in the presence of decoherence.

Decoherence. While we have shown that the XX model outperforms the Ising model under ideal conditions, it remains to be seen whether this advantage persists in the presence of relevant decoherence processes found in experiments. There are two key distinctions regarding the effects of decoherence in the two models. First, the XX model is realized in a rotating frame, in which the decoherence takes on a different form. Second, $t_{\rm opt}$ is typically much longer for the XX model, owing to both the factor-of-two reduction in the interaction strength in the XX model relative to the Ising model and the ability of the XX model to sustain a continued improvement in the squeezing over comparatively longer times (scaled by the average interaction strength) as a result of the many-body gap. As such, the XX model will generically be more susceptible to decoherence.

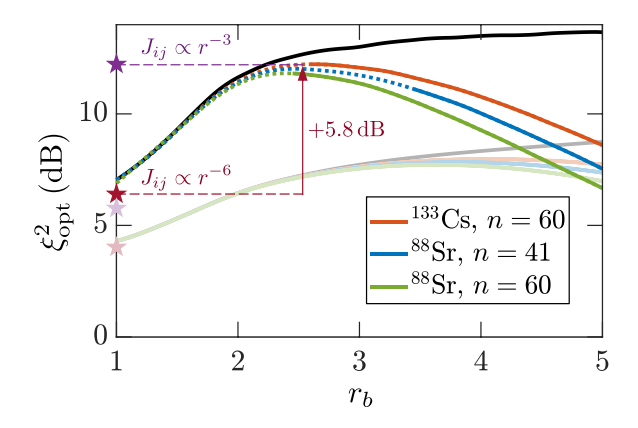


FIG. 3. Maximum attainable spin squeezing vs r_b generated by the XX model when incoherent effects are taken into account compared to the ideal case without decoherence (black, solid). We show results for a 14×14 lattice with $\gamma_- = \gamma_d = f \gamma_r/2$ and f = 0.01. The dotted continuations of each solid line denote the r_b for which the RWA is not expected to be valid for current experimentally achievable transverse fields B. We also compare to the ideal spin squeezing for pure power-law dipolar (purple star) and vdW (red star) interactions. The analogous faded lines/symbols denote the corresponding results for Ising interactions.

The dominant form of decoherence arises from decay of the Rydberg state $|r\rangle$ or decay of $|e\rangle$. For Rydberg decay, there are two scenarios we consider: decay to $|g\rangle$ (γ_{rg}) and decay to $|e\rangle$ (γ_{re}). For the former, this will correspond to dissipation from $|d\rangle$ to $|g\rangle$ at rate $f\gamma_{rg}$; for the latter, this will correspond to an effective dephasing of rate $f\gamma_{re}$. For dissipation from $|e\rangle$ at rate γ_{eg} , this will correspond to decay from $|d\rangle$ to $|g\rangle$ at rate $(1-f)\gamma_{eg}$.

In the resulting effective spin-1/2 system, we include the effects of all three forms of decoherence via the Lindblad master equation,

$$\dot{\rho} = -i[H, \rho] + \sum_{\mu} \gamma_{\mu} \mathcal{D}_{\mu}[\rho], \tag{5a}$$

$$\mathcal{D}_{\mu}[\rho] \equiv \sum_{i} \left[l_{\mu,i} \rho l_{\mu,i}^{\dagger} - \frac{1}{2} \{ \rho, l_{\mu,i}^{\dagger} l_{\mu,i} \} \right], \tag{5b}$$

where $\mathcal{D}_{\mu}[\rho]$ describes a Lindbladian evolution term with rate γ_{μ} and Lindblad jump operator l_{μ} . In the effective two-level system, there is decay at rate $\gamma_{-} = f\gamma_{rg} + (1-f)\gamma_{eg}$, with $l_{-} = s^{-}$, and dephasing at rate $\gamma_{d} = f\gamma_{re}$, with $l_{d} \equiv n_{i} = 1/2 + s_{i}^{z}$. In the rotating frame, the system dephases in the transverse field direction at a rate γ_{-} and in the two orthogonal directions at a rate $(\gamma_{-} + \gamma_{d})/2$ with Lindblad jump operators s_{x} and $s_{y,z}$, respectively (see Supplemental Material [60]).

For Ising interactions, it is possible to solve Eq. (5) exactly [71]. For the XX model, we adapt a dissipative generalization of DTWA [72,73], which amounts to including fluctuations from dissipation via stochastic noise terms ([74] and Supplemental Material [60]). In Fig. 3, we compare ξ_{opt}^2 in the Ising and XX models in the presence of decoherence in a 14×14 lattice as a function of r_b for several Rydberg states (see Supplemental Material [60]). The relative values of γ_- and γ_d will depend on the choice of Rydberg state, branching ratios, and the temperature of the system. For simplicity, we

take $\gamma_- = \gamma_d = f \gamma_r / 2$, where γ_r is the total decay rate of $|r\rangle$ at T = 300 K to all states; a more complete treatment would take into account branching ratios and losses to states outside the manifold we consider, but this likely affects both Ising and XX implementations in a similar way. We also compare to $\xi_{\rm opt}^2$ attainable with power-law interactions in the absence of decoherence. The reason for comparing to the ideal vdW XX model is to demonstrate that the improved performance of the proposed scheme is not a consequence of the power-law tail, but instead it is a combination of the soft core and the gap protection. The comparison to the dipolar XX model is to illustrate that the performance is comparable to that of a truly long-range model.

We see in Fig. 3 that the soft-core XX model generates significantly more squeezing than the other models, with only fully coherent, gap-protected long-range dipolar interactions realizing comparable squeezing. While increasing r_b nominally improves squeezing, here the role of decoherence becomes dominant at large r_b , and the best performance occurs for some optimal $r_b < L$. Moreover, unlike the soft-core Ising model whose optimal performance occurs near $r_b \approx 3$ –5, the soft-core XX model performs best for $r_b \approx 2$ –3, which is more experimentally feasible [51,52,54,55] due to practical limitations on the size of r_b imposed by the onset of blackbody radiation-induced avalanche processes [75–80].

A scaling analysis indicates that $\bar{J} \sim J_0 r_b^D \sim f^2 n^{*-3} r_b^{D-6}$ (see Supplemental Material [60]), where n^* is the effective principal quantum number, so decreasing f, increasing n^* , or increasing r_b reduces the requisite transverse field for the RWA to remain valid. Additionally, noting that $\gamma_r \approx A n^{*-3} + B n^{*-2}$, where A and B correspond to contributions from spontaneous emission and blackbody radiation, respectively, then $f \gamma_r / \bar{J} \sim (A + B n^*) r_b^{6-D} / f$, so the decoherence becomes more relevant with decreasing f, increasing n^* , or increasing r_b . For typical Rydberg states, $B n^* < A$, so the dependence on n^* is relatively small. The observation that increasing r_b is not beneficial is fundamentally connected to the relevance of blackbody radiation at large r_b , and therefore the relatively minimal effect of decoherence at the optimal r_b for soft-core interactions ensures the avalanche processes can be mitigated.

Outlook. Overall, we find that the soft-core XX model strongly outperforms other natural squeezing protocols for a wide range of experimental parameters and atoms, paving the way for generically realizing gap-protected enhanced squeezing in Rydberg platforms. Although we have focused on spin squeezing with Rydberg atoms, the driving idea discussed here can potentially be used in other systems with finite-range interactions. For example, since even an interaction range of two sites is sufficient to realize significant enhancements in the squeezing, circuit-QED systems with interactions beyond nearest neighbor may benefit from this approach [81,82]. From a theoretical point of view, a comprehensive examination of the various scaling behaviors with r_b and how they depend on the dimension, power-law tail, and system size, as well as any potential connection between the scaling with the presence Anderson's tower of states [83], would be very illuminating. Additionally, the work here provides a foundation for developing more sophisticated protocols, including Floquet engineering [54,84-88] or variational algorithms [89–91], which might take further advantage of the combination of a soft-core potential with gap protection and generate even better and more robust spin squeezing.

We thank P. Rabl, J. Huber, and T. Roscilde for helpful discussions as well as W. F. McGrew and D. Wellnitz for a careful reading and comments on the manuscript. This work

is supported by the AFOSR Grant No. FA9550-19-1-0275, by the NSF JILA-PFC PHY-1734006, QLCI-OMA-2016244, by the U.S. Department of Energy, Office of Science, National Quantum Information Science Research Centers Quantum Systems Accelerator, and by NIST. J.T.Y. was supported in part by the NIST NRC Postdoctoral Research Associateship Award

- V. Giovannetti, S. Lloyd, and L. Maccone, Quantum Metrology, Phys. Rev. Lett. 96, 010401 (2006).
- [2] V. Giovannetti, S. Lloyd, and L. Maccone, Advances in quantum metrology, Nat. Photon. 5, 222 (2011).
- [3] G. Tóth and I. Apellaniz, Quantum metrology from a quantum information science perspective, J. Phys. A 47, 424006 (2014).
- [4] M. Szczykulska, T. Baumgratz, and A. Datta, Multi-parameter quantum metrology, Adv. Phys. X 1, 621 (2016).
- [5] L. Pezzè, A. Smerzi, M. K. Oberthaler, R. Schmied, and P. Treutlein, Quantum metrology with nonclassical states of atomic ensembles, Rev. Mod. Phys. 90, 035005 (2018).
- [6] T. Bothwell, C. J. Kennedy, A. Aeppli, D. Kedar, J. M. Robinson, E. Oelker, A. Staron, and J. Ye, Resolving the gravitational redshift across a millimetre-scale atomic sample, Nature (London) 602, 420 (2022).
- [7] X. Zheng, J. Dolde, V. Lochab, B. N. Merriman, H. Li, and S. Kolkowitz, Differential clock comparisons with a multiplexed optical lattice clock, Nature (London) 602, 425 (2022).
- [8] K. Beloy, M. I. Bodine, T. Bothwell, S. M. Brewer, S. L. Bromley, J. S. Chen, J. D. Deschênes, S. A. Diddams, R. J. Fasano, T. M. Fortier, Y. S. Hassan, D. B. Hume, D. Kedar, C. J. Kennedy, I. Khader, A. Koepke, D. R. Leibrandt, H. Leopardi, A. D. Ludlow, W. F. McGrew, W. R. Milner, N. R. Newbury, D. Nicolodi, E. Oelker, T. E. Parker, J. M. Robinson, S. Romisch, S. A. Schäffer, J. A. Sherman, L. C. Sinclair, L. Sonderhouse, W. C. Swann, J. Yao, J. Ye, and X. Zhang, Frequency ratio measurements at 18-digit accuracy using an optical clock network, Nature (London) 591, 564 (2021).
- [9] S. M. Brewer, J.-S. Chen, A. M. Hankin, E. R. Clements, C. W. Chou, D. J. Wineland, D. B. Hume, and D. R. Leibrandt, ²⁷Al⁺ Quantum-Logic Clock with a Systematic Uncertainty Below 10⁻¹⁸, Phys. Rev. Lett. 123, 033201 (2019).
- [10] I. S. Madjarov, A. Cooper, A. L. Shaw, J. P. Covey, V. Schkolnik, T. H. Yoon, J. R. Williams, and M. Endres, An Atomic-Array Optical Clock with Single-Atom Readout, Phys. Rev. X 9, 041052 (2019).
- [11] M. A. Norcia, A. W. Young, W. J. Eckner, E. Oelker, J. Ye, and A. M. Kaufman, Seconds-scale coherence on an optical clock transition in a tweezer array, Science **366**, 93 (2019).
- [12] A. W. Young, W. J. Eckner, W. R. Milner, D. Kedar, M. A. Norcia, E. Oelker, N. Schine, J. Ye, and A. M. Kaufman, Halfminute-scale atomic coherence and high relative stability in a tweezer clock, Nature (London) 588, 408 (2020).
- [13] W. Lee, H. Kim, and J. Ahn, Three-dimensional rearrangement of single atoms using actively controlled optical microtraps, Opt. Express 24, 9816 (2016).
- [14] D. Barredo, S. de Léséleuc, V. Lienhard, T. Lahaye, and A. Browaeys, An atom-by-atom assembler of defect-free arbitrary two-dimensional atomic arrays, Science **354**, 1021 (2016).

- [15] M. Endres, H. Bernien, A. Keesling, H. Levine, E. R. Anschuetz, A. Krajenbrink, C. Senko, V. Vuletic, M. Greiner, and M. D. Lukin, Atom-by-atom assembly of defect-free one-dimensional cold atom arrays, Science 354, 1024 (2016).
- [16] M. A. Norcia, A. W. Young, and A. M. Kaufman, Microscopic Control and Detection of Ultracold Strontium in Optical-Tweezer Arrays, Phys. Rev. X 8, 041054 (2018).
- [17] A. Browaeys and T. Lahaye, Many-body physics with individually controlled Rydberg atoms, Nat. Phys. 16, 132 (2020).
- [18] D. Bluvstein, A. Omran, H. Levine, A. Keesling, G. Semeghini, S. Ebadi, T. T. Wang, A. A. Michailidis, N. Maskara, W. W. Ho, S. Choi, M. Serbyn, M. Greiner, V. Vuletić, and M. D. Lukin, Controlling quantum many-body dynamics in driven Rydberg atom arrays, Science 371, 1355 (2021).
- [19] C. W. Chou, D. B. Hume, J. C. J. Koelemeij, D. J. Wineland, and T. Rosenband, Frequency Comparison of Two High-Accuracy Al⁺ Optical Clocks, Phys. Rev. Lett. 104, 070802 (2010).
- [20] P. O. Schmidt, T. Rosenband, C. Langer, W. M. Itano, J. C. Bergquist, and D. J. Wineland, Spectroscopy using quantum logic, Science 309, 749 (2005).
- [21] M. Saffman, T. G. Walker, and K. Mølmer, Quantum information with Rydberg atoms, Rev. Mod. Phys. 82, 2313 (2010).
- [22] M. Saffman, Quantum computing with atomic qubits and Rydberg interactions: progress and challenges, J. Phys. B 49, 202001 (2016).
- [23] X. Wu, X. Liang, Y. Tian, F. Yang, C. Chen, Y.-C. Liu, M. K. Tey, and L. You, A concise review of Rydberg atom based quantum computation and quantum simulation, Chinese Phys. B 30, 020305 (2021).
- [24] M. Morgado and S. Whitlock, Quantum simulation and computing with Rydberg-interacting qubits, AVS Quantum Sci. 3, 023501 (2021).
- [25] M. Kitagawa and M. Ueda, Squeezed spin states, Phys. Rev. A 47, 5138 (1993).
- [26] D. J. Wineland, J. J. Bollinger, W. M. Itano, F. L. Moore, and D. J. Heinzen, Spin squeezing and reduced quantum noise in spectroscopy, Phys. Rev. A 46, R6797 (1992).
- [27] D. J. Wineland, J. J. Bollinger, W. M. Itano, and D. J. Heinzen, Squeezed atomic states and projection noise in spectroscopy, Phys. Rev. A **50**, 67 (1994).
- [28] M. Foss-Feig, Z.-X. Gong, A. V. Gorshkov, and C. W. Clark, Entanglement and spin-squeezing without infinite-range interactions, arXiv:1612.07805 (2016).
- [29] M. A. Perlin, C. Qu, and A. M. Rey, Spin Squeezing with Short-Range Spin-Exchange Interactions, Phys. Rev. Lett. 125, 223401 (2020).
- [30] M. Block, B. Ye, B. Roberts, S. Chern, W. Wu, Z. Wang, L. Pollet, E. J. Davis, B. I. Halperin, and N. Y. Yao, A Universal Theory of Spin Squeezing, arXiv:2301.09636 (2023).

- [31] F. Piéchon, J. N. Fuchs, and F. Laloë, Cumulative Identical Spin Rotation Effects in Collisionless Trapped Atomic Gases, Phys. Rev. Lett. **102**, 215301 (2009).
- [32] X. Du, Y. Zhang, J. Petricka, and J. E. Thomas, Controlling Spin Current in a Trapped Fermi Gas, Phys. Rev. Lett. **103**, 010401 (2009).
- [33] C. Deutsch, F. Ramirez-Martinez, C. Lacroûte, F. Reinhard, T. Schneider, J. N. Fuchs, F. Piéchon, F. Laloë, J. Reichel, and P. Rosenbusch, Spin Self-Rephasing and Very Long Coherence Times in a Trapped Atomic Ensemble, Phys. Rev. Lett. 105, 020401 (2010).
- [34] X. Zhang, M. Bishof, S. L. Bromley, C. V. Kraus, M. S. Safronova, P. Zoller, A. M. Rey, and J. Ye, Spectroscopic observation of SU(*N*)-symmetric interactions in Sr orbital magnetism, Science **345**, 1467 (2014).
- [35] A. Rey, A. Gorshkov, C. Kraus, M. Martin, M. Bishof, M. Swallows, X. Zhang, C. Benko, J. Ye, N. Lemke, and A. Ludlow, Probing many-body interactions in an optical lattice clock, Ann. Phys. (NY) 340, 311 (2014).
- [36] C. Solaro, A. Bonnin, F. Combes, M. Lopez, X. Alauze, J.-N. Fuchs, F. Piéchon, and F. Pereira Dos Santos, Competition between Spin Echo and Spin Self-Rephasing in a Trapped Atom Interferometer, Phys. Rev. Lett. 117, 163003 (2016).
- [37] A. P. Koller, M. L. Wall, J. Mundinger, and A. M. Rey, Dynamics of Interacting Fermions in Spin-Dependent Potentials, Phys. Rev. Lett. 117, 195302 (2016).
- [38] S. L. Bromley, S. Kolkowitz, T. Bothwell, D. Kedar, A. Safavi-Naini, M. L. Wall, C. Salomon, A. M. Rey, and J. Ye, Dynamics of interacting fermions under spin-orbit coupling in an optical lattice clock, Nat. Phys. 14, 399 (2018).
- [39] M. A. Norcia, R. J. Lewis-Swan, J. R. K. Cline, B. Zhu, A. M. Rey, and J. K. Thompson, Cavity-mediated collective spin-exchange interactions in a strontium superradiant laser, Science **361**, 259 (2018).
- [40] M. J. Martin, M. Bishof, M. D. Swallows, X. Zhang, C. Benko, J. Von-Stecher, A. V. Gorshkov, A. M. Rey, and J. Ye, A quantum many-body spin system in an optical lattice clock, Science **341**, 632 (2013).
- [41] S. Smale, P. He, B. A. Olsen, K. G. Jackson, H. Sharum, S. Trotzky, J. Marino, A. M. Rey, and J. H. Thywissen, Observation of a transition between dynamical phases in a quantum degenerate Fermi gas, Sci. Adv. 5, eaax1568 (2019).
- [42] P. He, M. A. Perlin, S. R. Muleady, R. J. Lewis-Swan, R. B. Hutson, J. Ye, and A. M. Rey, Engineering spin squeezing in a 3D optical lattice with interacting spin-orbit-coupled fermions, Phys. Rev. Res. 1, 033075 (2019).
- [43] E. J. Davis, A. Periwal, E. S. Cooper, G. Bentsen, S. J. Evered, K. Van Kirk, and M. H. Schleier-Smith, Protecting Spin Coherence in a Tunable Heisenberg Model, Phys. Rev. Lett. 125, 060402 (2020).
- [44] M. A. Perlin, D. Barberena, M. Mamaev, B. Sundar, R. J. Lewis-Swan, and A. M. Rey, Engineering infinite-range SU(*n*) interactions with spin-orbit-coupled fermions in an optical lattice, Phys. Rev. A **105**, 023326 (2022).
- [45] J. Ma, X. Wang, C. Sun, and F. Nori, Quantum spin squeezing, Phys. Rep. 509, 89 (2011).
- [46] L. I. R. Gil, R. Mukherjee, E. M. Bridge, M. P. A. Jones, and T. Pohl, Spin Squeezing in a Rydberg Lattice Clock, Phys. Rev. Lett. 112, 103601 (2014).

- [47] G. Pupillo, A. Micheli, M. Boninsegni, I. Lesanovsky, and P. Zoller, Strongly Correlated Gases of Rydberg-Dressed Atoms: Quantum and Classical Dynamics, Phys. Rev. Lett. 104, 223002 (2010).
- [48] J. E. Johnson and S. L. Rolston, Interactions between Rydberg-dressed atoms, Phys. Rev. A 82, 033412 (2010).
- [49] N. Henkel, R. Nath, and T. Pohl, Three-Dimensional Roton Excitations and Supersolid Formation in Rydberg-Excited Bose-Einstein Condensates, Phys. Rev. Lett. 104, 195302 (2010).
- [50] Y.-Y. Jau, A. M. Hankin, T. Keating, I. H. Deutsch, and G. W. Biedermann, Entangling atomic spins with a Rydberg-dressed spin-flip blockade, Nat. Phys. 12, 71 (2016).
- [51] J. Zeiher, R. van Bijnen, P. Schauß, S. Hild, J.-Y. Choi, T. Pohl, I. Bloch, and C. Gross, Many-body interferometry of a Rydberg-dressed spin lattice, Nat. Phys. 12, 1095 (2016).
- [52] J. Zeiher, J.-y. Choi, A. Rubio-Abadal, T. Pohl, R. van Bijnen, I. Bloch, and C. Gross, Coherent Many-Body Spin Dynamics in a Long-Range Interacting Ising Chain, Phys. Rev. X 7, 041063 (2017).
- [53] A. Arias, G. Lochead, T. M. Wintermantel, S. Helmrich, and S. Whitlock, Realization of a Rydberg-Dressed Ramsey Interferometer and Electrometer, Phys. Rev. Lett. 122, 053601 (2019).
- [54] V. Borish, O. Marković, J. A. Hines, S. V. Rajagopal, and M. Schleier-Smith, Transverse-Field Ising Dynamics in a Rydberg-Dressed Atomic Gas, Phys. Rev. Lett. 124, 063601 (2020).
- [55] E. Guardado-Sanchez, B. M. Spar, P. Schauss, R. Belyansky, J. T. Young, P. Bienias, A. V. Gorshkov, T. Iadecola, and W. S. Bakr, Quench Dynamics of a Fermi Gas with Strong Nonlocal Interactions, Phys. Rev. X 11, 021036 (2021).
- [56] N. Schine, A. W. Young, W. J. Eckner, M. J. Martin, and A. M. Kaufman, Long-lived Bell states in an array of optical clock qubits, Nat. Phys. 18, 1067 (2022).
- [57] M. J. Martin, Y.-Y. Jau, J. Lee, A. Mitra, I. H. Deutsch, and G. W. Biedermann, A Mølmer-Sørensen Gate with Rydberg-Dressed Atoms, arXiv:2111.14677 (2021).
- [58] M. Khazali, H. W. Lau, A. Humeniuk, and C. Simon, Large energy superpositions via Rydberg dressing, Phys. Rev. A 94, 023408 (2016).
- [59] M. Khazali, Progress towards macroscopic spin and mechanical superposition via Rydberg interaction, Phys. Rev. A 98, 043836 (2018).
- [60] See Supplemental Material at http://link.aps.org/supplemental/ 10.1103/PhysRevResearch.5.L012033 doi for details on the effect of a finite transverse field on squeezing dynamics, benchmarking DTWA in 1D, the experimental parameters used in Fig. 3, and the implementation of dissipative DTWA.
- [61] P. Jurcevic, B. P. Lanyon, P. Hauke, C. Hempel, P. Zoller, R. Blatt, and C. F. Roos, Quasiparticle engineering and entanglement propagation in a quantum many-body system, Nature (London) 511, 202 (2014).
- [62] P. Richerme, Z. X. Gong, A. Lee, C. Senko, J. Smith, M. Foss-Feig, S. Michalakis, A. V. Gorshkov, and C. Monroe, Non-local propagation of correlations in quantum systems with long-range interactions, Nature (London) 511, 198 (2014).
- [63] M. L. Wall, A. Safavi-Naini, and A. M. Rey, Boson-mediated quantum spin simulators in transverse fields: *XY* model and spin-boson entanglement, Phys. Rev. A **95**, 013602 (2017).

- [64] T. G. Kiely and J. K. Freericks, Relationship between the transverse-field Ising model and the *XY* model via the rotating-wave approximation, Phys. Rev. A **97**, 023611 (2018).
- [65] N. Friis, O. Marty, C. Maier, C. Hempel, M. Holzäpfel, P. Jurcevic, M. B. Plenio, M. Huber, C. Roos, R. Blatt, and B. Lanyon, Observation of Entangled States of a Fully Controlled 20-Qubit System, Phys. Rev. X 8, 021012 (2018).
- [66] C. Monroe, W. C. Campbell, L.-M. Duan, Z.-X. Gong, A. V. Gorshkov, P. W. Hess, R. Islam, K. Kim, N. M. Linke, G. Pagano, P. Richerme, C. Senko, and N. Y. Yao, Programmable quantum simulations of spin systems with trapped ions, Rev. Mod. Phys. 93, 025001 (2021).
- [67] J. Schachenmayer, A. Pikovski, and A. M. Rey, Many-Body Quantum Spin Dynamics with Monte Carlo Trajectories on a Discrete Phase Space, Phys. Rev. X 5, 011022 (2015).
- [68] J. Schachenmayer, A. Pikovski, and A. M. Rey, Dynamics of correlations in two-dimensional quantum spin models with long-range interactions: A phase-space Monte Carlo study, New J. Phys. 17, 065009 (2015).
- [69] B. Zhu, A. M. Rey, and J. Schachenmayer, A generalized phase space approach for solving quantum spin dynamics, New J. Phys. 21, 082001 (2019).
- [70] S. R. Muleady, M. Yang, S. R. White, and A. M. Rey (unpublished)..
- [71] M. Foss-Feig, K. R. A. Hazzard, J. J. Bollinger, and A. M. Rey, Nonequilibrium dynamics of arbitrary-range Ising models with decoherence: An exact analytic solution, Phys. Rev. A 87, 042101 (2013).
- [72] J. Huber, A. M. Rey, and P. Rabl, Realistic simulations of spin squeezing and cooperative coupling effects in large ensembles of interacting two-level systems, Phys. Rev. A 105, 013716 (2022).
- [73] V. P. Singh and H. Weimer, Driven-Dissipative Criticality within the Discrete Truncated Wigner Approximation, Phys. Rev. Lett. 128, 200602 (2022).
- [74] D. Barberena, S. R. Muleady, J. J. Bollinger, R. J. Lewis-Swan, and A. M. Rey, Fast generation of spin squeezing via resonant spin-boson coupling (unpublished).
- [75] E. A. Goldschmidt, T. Boulier, R. C. Brown, S. B. Koller, J. T. Young, A. V. Gorshkov, S. L. Rolston, and J. V. Porto, Anomalous Broadening in Driven Dissipative Rydberg Systems, Phys. Rev. Lett. 116, 113001 (2016).
- [76] J. A. Aman, B. J. DeSalvo, F. B. Dunning, T. C. Killian, S. Yoshida, and J. Burgdörfer, Trap losses induced by nearresonant Rydberg dressing of cold atomic gases, Phys. Rev. A 93, 043425 (2016).
- [77] T. Boulier, E. Magnan, C. Bracamontes, J. Maslek, E. A. Goldschmidt, J. T. Young, A. V. Gorshkov, S. L. Rolston, and J. V. Porto, Spontaneous avalanche dephasing in large Rydberg ensembles, Phys. Rev. A 96, 053409 (2017).
- [78] J. T. Young, T. Boulier, E. Magnan, E. A. Goldschmidt, R. M. Wilson, S. L. Rolston, J. V. Porto, and A. V. Gorshkov, Dissipation-induced dipole blockade and antiblockade in driven Rydberg systems, Phys. Rev. A 97, 023424 (2018).

- [79] J. De Hond, N. Cisternas, R. J. Spreeuw, H. B. Van Linden Van Den Heuvell, and N. J. Druten, Interplay between van der Waals and dipole-dipole interactions among Rydberg atoms, J. Phys. B 53, 084007 (2020).
- [80] L. Festa, N. Lorenz, L.-M. Steinert, Z. Chen, P. Osterholz, R. Eberhard, and C. Gross, Blackbody-radiation-induced facilitated excitation of Rydberg atoms in optical tweezers, Phys. Rev. A 105, 013109 (2022).
- [81] C. Song, K. Xu, H. Li, Y. R. Zhang, X. Zhang, W. Liu, Q. Guo, Z. Wang, W. Ren, J. Hao, H. Feng, H. Fan, D. Zheng, D. W. Wang, H. Wang, and S. Y. Zhu, Generation of multicomponent atomic Schrödinger cat states of up to 20 qubits, Science 365, 574 (2019).
- [82] P. Groszkowski, M. Koppenhöfer, H.-K. Lau, and A. A. Clerk, Reservoir-Engineered Spin Squeezing: Macroscopic Even-Odd Effects and Hybrid-Systems Implementations, Phys. Rev. X 12, 011015 (2022).
- [83] T. Comparin, F. Mezzacapo, and T. Roscilde, Robust spin squeezing from the tower of states of U(1)-symmetric spin Hamiltonians, Phys. Rev. A 105, 022625 (2022).
- [84] L. M. K. Vandersypen and I. L. Chuang, NMR techniques for quantum control and computation, Rev. Mod. Phys. 76, 1037 (2005).
- [85] J. Choi, H. Zhou, H. S. Knowles, R. Landig, S. Choi, and M. D. Lukin, Robust Dynamic Hamiltonian Engineering of Many-Body Spin Systems, Phys. Rev. X 10, 031002 (2020).
- [86] H. Zhou, J. Choi, S. Choi, R. Landig, A. M. Douglas, J. Isoya, F. Jelezko, S. Onoda, H. Sumiya, P. Cappellaro, H. S. Knowles, H. Park, and M. D. Lukin, Quantum Metrology with Strongly Interacting Spin Systems, Phys. Rev. X 10, 031003 (2020).
- [87] S. Geier, N. Thaicharoen, C. Hainaut, T. Franz, A. Salzinger, A. Tebben, D. Grimshandl, G. Zürn, and M. Weidemüller, Floquet Hamiltonian engineering of an isolated many-body spin system, Science 374, 1149 (2021).
- [88] P. Scholl, H. J. Williams, G. Bornet, F. Wallner, D. Barredo, L. Henriet, A. Signoles, C. Hainaut, T. Franz, S. Geier, A. Tebben, A. Salzinger, G. Zürn, T. Lahaye, M. Weidemüller, and A. Browaeys, Microwave engineering of programmable XXZ Hamiltonians in arrays of Rydberg atoms, PRX Quantum 3, 020303 (2022).
- [89] R. Kaubruegger, P. Silvi, C. Kokail, R. van Bijnen, A. M. Rey, J. Ye, A. M. Kaufman, and P. Zoller, Variational Spin-Squeezing Algorithms on Programmable Quantum Sensors, Phys. Rev. Lett. 123, 260505 (2019).
- [90] R. Kaubruegger, D. V. Vasilyev, M. Schulte, K. Hammerer, and P. Zoller, Quantum Variational Optimization of Ramsey Interferometry and Atomic Clocks, Phys. Rev. X 11, 041045 (2021).
- [91] C. D. Marciniak, T. Feldker, I. Pogorelov, R. Kaubruegger, D. V. Vasilyev, R. van Bijnen, P. Schindler, P. Zoller, R. Blatt, and T. Monz, Optimal metrology with programmable quantum sensors, Nature (London) 603, 604 (2022).